ICIC Express Letters
Volume **18**, Number **3**, March **2024**
ICIC International ©2024 ISSN 1881-803X
pp. **229–234**

QUALITY IMPROVEMENT OF CELL-LIKE IMAGES GENERATED USING INVERSE IRIS FILTER

Toru Hiraoka[1] and Seiichi Hamasaki[2]

[1]Department of Information Systems
University of Nagasaki
1-1-1, Manabino, Nagayo-chou, Nishisonogi-gun, Nagasaki-ken 851-2195, Japan
hiraoka@sun.ac.jp

[2]Nagasaki Prefectural Government
3-1, Onoue-machi, Nagasaki-shi, Nagasaki-ken 850-0058, Japan
hamasaki_s970@pref.nagasaki.lg.jp

Received May 2023; accepted July 2023

Abstract. *A non-photorealistic rendering method has been proposed to automatically generate cell-like images from photographic images by an iterative process using inverse iris filter. Cell-like images are expressed by superimposing cell-like patterns that imitate the cell membrane and cell nucleus on the photographic images. However, cell-like images generated by the conventional method have areas where cell-like patterns are unlikely to occur, and the shape of cell-like patterns does not change much. In this paper, we improve the appearance of cell-like images by reducing the areas that are unlikely to occur and changing the shapes of cell-like patterns. Our method extends the conventional method to use multiple radii. To validate the effectiveness of our method, we conducted an experiment using various photographic images. Additionally, we conducted an experiment to visually confirm cell-like patterns that change when the value of the parameters added by our method is changed.*
Keywords: Non-photorealistic rendering, Cell, Inverse iris filter, Multiple radii, Quality improvement

1. **Introduction.** Many studies have been done on non-photorealistic rendering [1, 2, 3, 4, 5, 6, 7, 8, 9]. Non-photorealistic rendering is a computer graphics technique [10] for converting photorealistic images into non-photorealistic images, and can imitate the painting styles of famous painters and cartoonists, or create unprecedented art expressions. A method of non-photorealistic rendering for unprecedented art expressions is proposed, which automatically generates cell-like images from photographic images [11]. Cell-like images are expressed by superimposing cell-like patterns that imitate the cell membrane and cell nucleus on the photographic images. The conventional method is executed by an iterative process using inverse iris filter. Inverse iris filter is a combination of iris filter [12, 13] and inverse filter [14, 15]. However, cell-like images generated by the conventional method have areas where cell-like patterns are unlikely to occur, and the size and shape of cell-like patterns do not change much. Therefore, methods for improving the appearance of cell-like images have also been proposed [16, 17, 18]: [16] emphasized aligned cell-like patterns by synthesizing sine and cosine waves into photographic images, [17] emphasized and aligned cell-like patterns along the edges by using Euclidean distance from the edges of photographic images, and [18] changed the size of cell-like patterns by using RGB-D images.

In this paper, we improve the appearance of cell-like images by reducing the areas that are unlikely to occur and changing the shapes of cell-like patterns. Our method is

DOI: 10.24507/icicel.18.03.229

executed by an iterative process using inverse iris filter with multiple radii. To verify the effectiveness of our method, we conducted an experiment using various photographic images. Additionally, we conducted an experiment to visually confirm cell-like patterns that change when the value of the parameter added by our method is changed. As a result of the experiments, it was found that our method can reduce the areas that are unlikely to occur and can change the shape of cell-like patterns by changing the value of the parameter.

This paper is organized as follows: the second section describes our method for generating cell-like images from photographic images, the third section shows experimental results and reveals the effectiveness of our method, and the conclusion of this paper is given in the fourth section.

2. **Our Method.** Our method was implemented in two steps: Step 1 is a process using iris filter with multiple radii, and Step 2 is a process using inverse filter. In Step 2, a process to generate cell-like patterns is added to the areas where cell-like patterns are unlikely to occur. Steps 1 and 2 are repeated, where the radii in Step 1 are changed according to the iteration number. A flow chart of our method is shown in Figure 1.

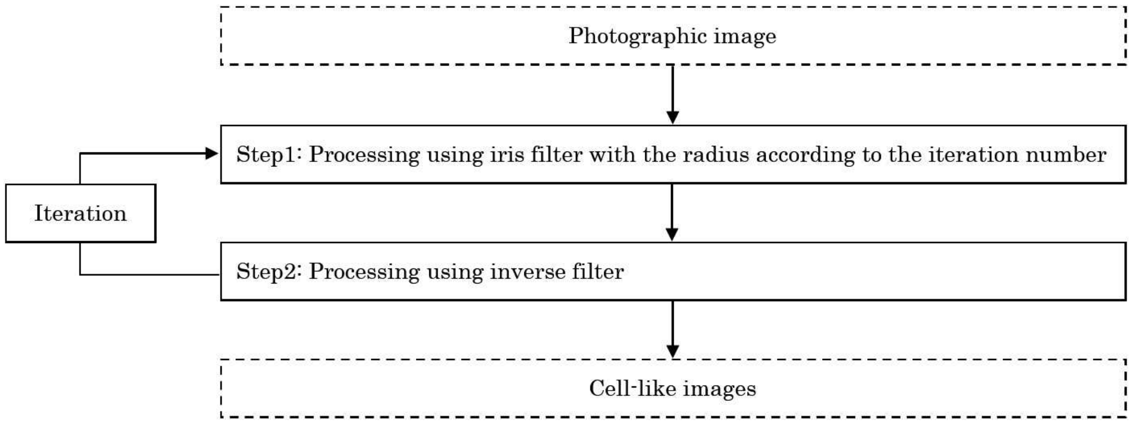

FIGURE 1. Flow chart of our method

Details of the steps in Figure 1 are explained below.

Step 0: Let input pixel values of RGB on color image coordinates (i, j) be $f_{R,i,j}$, $f_{G,i,j}$ and $f_{B,i,j}$. The pixel values $f_{R,i,j}$, $f_{G,i,j}$ and $f_{B,i,j}$ have value of U gradation from 0 to $U-1$. The gray scale pixel values $f_{i,j}$ are calculated by the following equation.

$$f_{i,j} = \frac{f_{R,i,j} + f_{G,i,j} + f_{B,i,j}}{3} \tag{1}$$

Then, let the pixel values of the image at the t-th iteration number be $f^{(0)}_{R,i,j}$, $f^{(0)}_{G,i,j}$, $f^{(0)}_{B,i,j}$ and $f^{(t)}_{i,j}$, where $f^{(0)}_{R,i,j} = f_{R,i,j}$, $f^{(0)}_{G,i,j} = f_{G,i,j}$ and $f^{(0)}_{B,i,j} = f_{B,i,j}$.

Step 1: Assuming that the basic radius used in iris filter is r and the number of the radii is N, the radius r_t used in the t-th iteration is calculated as follows:

$$r_t = r(((t-1) \bmod N) + 1) \tag{2}$$

where mod represents the remainder operation.

Let output pixel value after the process with iris filter on $f^{(t)}_{i,j}$ be $IF\left(f^{(t)}_{i,j}\right)$. Iris filter is executed with the peripheral pixels (k, l) in the radius r_t from the target pixel (i, j). Compute the angles $\theta^{(t)}_{i,j,k,l}$ between a vector $(i-k, j-l)$ from the peripheral pixels (k, l) to the target pixel (i, j) and a vector $\left(\left(f^{(t)}_{k+2,l+2} + f^{(t)}_{k+2,l+1} + f^{(t)}_{k+2,l} + f^{(t)}_{k+2,l-1} + f^{(t)}_{k+2,l-2}\right) - \left(f^{(t)}_{k-2,l+2} + f^{(t)}_{k-2,l+1} + f^{(t)}_{k-2,l} + f^{(t)}_{k-2,l-1} + f^{(t)}_{k-2,l-2}\right), \left(f^{(t)}_{k+2,l+2} + f^{(t)}_{k+1,l+2} +\right.\right.$

$f^{(t)}_{k,l+2} + f^{(t)}_{k-1,l+2} + f^{(t)}_{k-2,l+2}\Big) - \Big(f^{(t)}_{k+2,l-2} + f^{(t)}_{k+1,l-2} + f^{(t)}_{k,l-2} + f^{(t)}_{k-1,l-2} + f^{(t)}_{k-2,l-2}\Big)\Big)$. Let the convergence indexes of the target pixel (i,j) be $c^{(t)}_{i,j}$. The convergence indexes $c^{(t)}_{i,j}$ are calculated by the following equation.

$$c^{(t)}_{i,j} = \frac{1}{S}\left|\sum_{k=i-r}^{i+r}\sum_{l=j-r}^{j+r}\cos\theta^{(t)}_{i,j,k,l}\right| \tag{3}$$

Let the minimum and maximum values of $c^{(t)}_{i,j}$ in all pixels be $c^{(t)}_{\min}$ and $c^{(t)}_{\max}$, respectively. Convert $c^{(t)}_{i,j}$ to $C^{(t)}_{i,j}$ by the following equation.

$$C^{(t)}_{i,j} = (U-1)\left(\frac{c^{(t)}_{i,j} - c^{(t)}_{\min}}{c^{(t)}_{\max} - c^{(t)}_{\min}}\right) \tag{4}$$

The values $IF\left(f^{(t)}_{i,j}\right)$ and $C^{(t)}_{i,j}$ are the same value.

Step 2: Compute the pixel values $f^{(t)}_{R,i,j}$, $f^{(t)}_{G,i,j}$ and $f^{(t)}_{B,i,j}$ by using inverse filter as

$$f^{(t)}_{R,i,j} = a\left(f^{(t-1)}_{i,j} - IF\left(f^{(t-1)}_{i,j}\right)\right) + f_{R,i,j} \tag{5}$$

$$f^{(t)}_{G,i,j} = a\left(f^{(t-1)}_{i,j} - IF\left(f^{(t-1)}_{i,j}\right)\right) + f_{G,i,j} \tag{6}$$

$$f^{(t)}_{B,i,j} = a\left(f^{(t-1)}_{i,j} - IF\left(f^{(t-1)}_{i,j}\right)\right) + f_{B,i,j} \tag{7}$$

$$f^{(t-1)}_{i,j} = \frac{f^{(t-1)}_{R,i,j} + f^{(t-1)}_{G,i,j} + f^{(t-1)}_{B,i,j}}{3} \tag{8}$$

where a is a positive constant less than or equal to 1. By the following equations, it is possible to generate cell-like patterns even in the areas where cell-like patterns are unlikely to occur.

$$f^{(t)}_{R,i,j} = \begin{cases} -f^{(t)}_{R,i,j} & \left(t \bmod N \neq 0 \ \wedge \ f^{(t)}_{R,i,j} < 0\right) \\ 2(U-1) - f^{(t)}_{R,i,j} & \left(t \bmod N \neq 0 \ \wedge \ f^{(t)}_{R,i,j} > U-1\right) \\ 0 & \left(t \bmod N = 0 \ \wedge \ f^{(t)}_{R,i,j} < 0\right) \\ U-1 & \left(t \bmod N = 0 \ \wedge \ f^{(t)}_{R,i,j} > U-1\right) \end{cases} \tag{9}$$

$$f^{(t)}_{G,i,j} = \begin{cases} -f^{(t)}_{G,i,j} & \left(t \bmod N \neq 0 \ \wedge \ f^{(t)}_{G,i,j} < 0\right) \\ 2(U-1) - f^{(t)}_{G,i,j} & \left(t \bmod N \neq 0 \ \wedge \ f^{(t)}_{G,i,j} > U-1\right) \\ 0 & \left(t \bmod N = 0 \ \wedge \ f^{(t)}_{G,i,j} < 0\right) \\ U-1 & \left(t \bmod N = 0 \ \wedge \ f^{(t)}_{G,i,j} > U-1\right) \end{cases} \tag{10}$$

$$f^{(t)}_{B,i,j} = \begin{cases} -f^{(t)}_{B,i,j} & \left(t \bmod N \neq 0 \ \wedge \ f^{(t)}_{B,i,j} < 0\right) \\ 2(U-1) - f^{(t)}_{B,i,j} & \left(t \bmod N \neq 0 \ \wedge \ f^{(t)}_{B,i,j} > U-1\right) \\ 0 & \left(t \bmod N = 0 \ \wedge \ f^{(t)}_{B,i,j} < 0\right) \\ U-1 & \left(t \bmod N = 0 \ \wedge \ f^{(t)}_{B,i,j} > U-1\right) \end{cases} \tag{11}$$

Repeat the process of Steps 1 and 2 NT times. The image composed of the pixel values $f^{(NT)}_{R,i,j}$, $f^{(NT)}_{G,i,j}$ and $f^{(NT)}_{B,i,j}$ is a cell-like image.

3. **Experiments.** We mainly conducted two experiments: the first experiment visually confirmed cell-like patterns generated by changing the newly added parameters, basic radius r and number of the radii N, using Lenna image shown in Figure 2, and the second experiment visually confirmed cell-like patterns generated from various photographic images shown in Figure 3. All photographic images used in the experiments were $512 * 512$ pixels and 256 gradation, and the values of the parameters a and T were set to 0.4 and 20 with reference to [11], respectively. As the value of a becomes bigger, the lines between cells representing the cell membrane become hard to see, but the regions representing the cell nucleus become clear. In [11], cell-like patterns were easy to see when the value of a was around 0.4. As the value of T becomes bigger, cell-like patterns become clear and cell-like images are converged. In [11], cell-like images converged when the value of T was around 20.

FIGURE 2. Lenna image

FIGURE 3. Various photographic images

3.1. **Experiment with changing the values of the parameters.** First, we assessed the variation in cell-like images generated by changing the number of the radii N with $r = 3$ in all cases using Lenna image. The results for $N = 1$, 2, 3, 4, 5, 6, 7 and 8 are shown in Figure 4. When the number of the radii N is 1, it is a cell-like image of the conventional method [11]. As the number of the radii N increased, the shape of cell-like patterns became more distorted and fine cell-like patterns were reduced. Additionally, compared with the cell-image (Figure 4(a)) of the conventional method [11], cell-like patterns became clearer in the whitish area in the lower right as the number of the radii N increased.

Next, we assessed the variation in cell-like images generated by changing the basic radius r with $N = 5$ in all cases using Lenna image. The results for $r = 1$, 2, 3 and 4 are shown in Figure 5. As the basic radius r increased, the size of cell-like patterns became larger and the shape of cell-like patterns became more distorted.

3.2. **Experiment with various photographic images.** We applied our method to four photographic images shown in Figure 4 with $r = 3$ and $N = 5$ in all cases. The results for four photographic images are shown in Figure 6. In all cases, cell-like patterns could be automatically generated on the whole image, and the shape of cell-like patterns could

(a) $N = 1$ (b) $N = 2$ (c) $N = 3$ (d) $N = 4$

(e) $N = 5$ (f) $N = 6$ (g) $N = 7$ (h) $N = 8$

FIGURE 4. Cell-like images with the number of the radii $N = 1$, 2, 3, 4, 5, 6, 7 and 8

(a) $r = 1$ (b) $r = 2$ (c) $r = 3$ (d) $r = 4$

FIGURE 5. Cell-like images with $r = 1$, 2, 3 and 4

FIGURE 6. Various cell-like images

be distorted. Additionally, cell-like patterns were also generated in the finely textured region (mandrill hair in the third image from the left).

4. **Conclusions.** We proposed a non-photorealistic rendering method to automatically generate cell-like images with reducing the areas that are unlikely to occur and distorting the shape of cell-like patterns from photographic images. Our method was executed by an iterative process using inverse iris filter with multiple radii. We demonstrated the

effectiveness of our method through two experimental sets: the first experimental set visually confirmed cell-like patterns generated by changing the number of the radii added by our method using Lenna image, and the second experimental set visually confirmed cell-like patterns generated from four photographic images. As a result of the experiments, it was found that our method can distort the shape of cell-like patterns and the shape of cell-like patterns can be changed by changing the number of the multiple radii. Additionally, it was found that cell-like patterns could be automatically generated on the whole image.

The future task is to expand our method for application to videos and three dimensional data.

Acknowledgment. This work was supported by JSPS KAKENHI Grant Number JP23K 11727 and The Telecommunications Advancement Foundation Grant.

REFERENCES

[1] P. Haeberli, Paint by numbers: Abstract image representations, *ACM SIGGRAPH Computer Graphics*, vol.24, no.4, pp.207-214, 1990.

[2] J. Lansdown and S. Schofield, Expressive rendering: A review of nonphotorealistic techniques, *IEEE Computer Graphics and Applications*, vol.15, no.3, pp.29-37, 1995.

[3] D.-L. Way, M.-K. Yang, Z.-C. Shih and R.-R. Lee, A colored pencil non-photorealistic rendering for 2D images, *International Journal of Innovative Computing, Information and Control*, vol.10, no.1, pp.233-241, 2014.

[4] J. Correia, L. Vieira, N. Rodriguez-Fernandez, J. Romero and P. Machado, Evolving image enhancement pipelines, *Artificial Intelligence in Music, Sound, Art and Design*, pp.82-97, 2021.

[5] P. L. Rosin, Y. K. Lai, D. Mould, R. Yi, I. Berger, L. Doyle, S. Lee, C. Li, Y. J. Liu, A. Semmo, A. Shamir, M. Son and H. Winnemoller, NPRportrait 1.0: A three-level benchmark for non-photorealistic rendering of portraits, *Computational Visual Media*, vol.8, no.3, pp.445-465, 2022.

[6] Y. Zhao, D. Ren, Y. Chen, W. Jia, R. Wang and X. Liu, Cartoon image processing: A survey, *International Journal of Computer Vision*, vol.130, no.11, pp.2733-2769, 2022.

[7] W. Ye, X. Zhu and Y. Liu, Multi-semantic preserving neural style transfer based on Y channel information of image, *The Visual Computer*, vol.39, no.2, pp.609-623, 2023.

[8] A. Karimov, E. Kopets, T. Shpilevaya, E. Katser, S. Leonov and D. Butusov, Comparing neural style transfer and gradient-based algorithms in brushstroke rendering tasks, *Mathematics*, vol.11, no.10, 2255, pp.1-30, DOI: 10.3390/math11102255, 2023.

[9] A. Ackerman, J. Auwaerter, E. Foulds, R. Page and E. Robinson, Cultural landscape visualization: The use of non-photorealistic 3D rendering as an analytical tool to convey change at statue of liberty national monument, *Journal of Cultural Heritage*, vol.62, pp.396-403, 2023.

[10] P. Sudkhot, K. W. Wong and C. Sombattheera, Collision avoidance and path planning in crowd simulation, *ICIC Express Letters*, vol.17, no.1, pp.13-24, 2023.

[11] T. Hiraoka, M. Hirota, K. Inoue and K. Urahama, Generating cell-like color images by inverse iris filter, *ICIC Express Letters*, vol.11, no.2, pp.399-404, 2017.

[12] H. Kobatake and S. Hashimoto, Convergence index filter for vector fields, *IEEE Transactions on Image Processing*, vol.8, no.8, pp.1029-1038, 1999.

[13] Y. Yoshinaga and H. Kobatake, Evaluation method of concentration degree and convergence index filter, *Medical Imaging Technology*, vol.19, no.3, pp.154-160, 2001.

[14] J. M. Ortega and W. C. Rheinboldt, Iterative solutions of nonlinear equations in several variables, *Society for Industrial Mathematics*, 1987.

[15] Z. Yu and K. Urahama, Iterative method for inverse nonlinear image processing, *IEICE Transactions on Fundamentals*, vol.E97-A, no.2, pp.719-721, 2014.

[16] T. Hiraoka, A method for emphasizing and aligning patterns in cell-like images, *ICIC Express Letters*, vol.13, no.11, pp.1031-1037, 2019.

[17] T. Hiraoka and K. Maeda, Generation of cell-like images using Euclidean distance from edge, *Journal of Robotics, Networking and Artificial Life*, vol.8, no.1, pp.14-17, 2021.

[18] T. Hiraoka, Generation of cell-like images with variable pattern size from RGB-D images, *ICIC Express Letters*, vol.16, no.7, pp.723-729, 2022.